Visual
Abstract

Fractographic characterization of Al_2O_{3p} particulates reinforced Al2014 alloy composites subjected to tensile loading

V. Bharath, V. Auradi

Dept. of Mechanical Engineering, Siddaganga Institute of Technology, Tumkur, Karnataka, India
bharathv88@gmail.com, http://orcid.org/0000-0001-6765-4728
vsauradi@gmail.com, http://orcid.org/0000-0001-6549-6340

M. Nagaral

Aircraft Research and Design Centre, Hindustan Aeronautics Limited, Bangalore, Karnataka, India
madev.nagaral@gmail.com, http://orcid.org/0000-0002-8248-7603

ABSTRACT. In the current investigation, efforts are being made to produce an Al2014-Al_2O_{3p} composite with an average particle size of 88 μm by liquid stir casting route. 9, 12 and 15 weight proportions of Al_2O_{3p} were added to the Al2014 base alloy. By using SEM and EDS testing, microstructural studies have been conducted. Al2014-9, 12 and 15 weight proportion of Al_2O_{3p} composites mechanical behavior is determined in line with ASTM standards. Electron microscopic images showed that alumina (Al_2O_{3p}) particles are dispersed uniformly within the Al2014 composite matrix. EDS study confirmed the proximity of Al and O elements to composites reinforced by Al_2O_{3p}. It is also found that Al2014-Al_2O_{3p} composite hardness, UTS, and yield strength are improved by the addition of 9, 12 and 15 weight proportion of Al_2O_{3p}. Due to the addition of alumina particles in the Al2014 matrix alloy, the ductility of the produced composites decreases. Tensile fractography is performed using SEM to consider the mechanisms for failure.

KEYWORDS. Al2014 alloy; Al_2O_{3p}; Mechanical Behavior; Fractography.

OPEN ACCESS

INTRODUCTION

Metal–matrix composites (MMCs) attract attention for applications like packing, substrates and support structure for electronic equipment and a variety of automotive components because of their comprehensive features such as low density, high rigidity, low thermal expansion coefficient, high thermal conductivity, high strength

and high use resistance [1–4]. The processing of alumina reinforced aluminium composite by casting process is particularly complex. The main reason is poor wettability of the alumina particles and agglomeration mechanism and this may likely to result in a poor mechanical strength and non-homogeneous dispersion. For the vast majority of the applications, consistent particle dispersion is fundamental to enhance the mechanical and wear properties. Stir casting (liquid metallurgy) has a number of significant points of interest. Some of them are as follows; (i) good bonding between the matrix and reinforcement (ii) easy to control the structure of the matrix (iii) ease of handling (iv) highly economic (v) closer net shape and the wide selection of materials and (vi) suitable for the production of composites reinforced with higher volume fraction of the particulates [3, 5, 6, 7]. Liquid state fabrication of MMC does comprise of two methods which rely upon the temperature at which the particles are brought into the melt. In melt stirring process, once the liquidus temperature of molten metal is accomplished the particles are infused into the melt, whereas in compo-casting strategy once the temperature of the base alloy reaches to semi solid state the particles are infused into it. In stir casting and compo-casting procedures, vortex produced is utilized for infuse the strengthening (reinforcing) particles. Nonetheless, the procedure of melting has two-vital problems, the most part of the ceramic particles are not wetted with the liquid matrix material and besides the particles will in general float or sink as per their comparative (relative) density with the liquid metal. Capacity of the melt to spread on a strong surface can be characterized as wettability. Wettability also refers the degree of close contact between the solid-liquid phases [8]. If the ceramic particles are poorly dispersed, it might increases the porosity and reduces the composite mechanical properties. This signifies a big challenge to create metal matrix composites. Low wettability implies the liquid matrix will not wet the surface of the strengthening particles subsequently they essentially drift on a superficial level attributable to surface tension, enormous surface space, maximum free energy of the surfaces at an interface and nearness of the oxide layer on the surface of the liquid metal. Enhancement in the wettability somewhat can be accomplished by many techniques such as mechanical stirring, heating up of the particles to expel the adsorbed gases from the surface of the particles [3], the increasing of alloying elements, utilization of the surface coating on the strengthening particles, and so on [9]. One more issue is the distribution (here afterwards distribution is referred as dissemination) of the strengthened particles in liquid matrix. Because of the density dissimilarity among the reinforcement and matrix, these particles in general drift or fix in the liquid matrix thus particles clustering/agglomeration take place [3]. It has been accounted for that infusion of particles with inert gas is useful in enhancing the dispersion [3]. M Kok [10] in his investigation on AA2024-alumina composites with three different sizes of the particles and weight percentages have seen by using electron microscopy the dissemination of the larger sizes of alumina particles are uniformly distributed while small (finer) particles resulting to the porosity and particles agglomeration. Hence, it is crucial to build up a strategy for creating aluminium metal matrix composites for the introduction and dispersion of strengthening particles in the liquid matrix and to accomplish a decent uniform dissemination of the particles in the matrix and the processing parameters relevant to the stir casting must be examined. Keeping the above perceptions in mind the present work is taken up to synthesize and characterize Al2014-alumina MMCs by varying weight percentages of the alumina particles by choosing optimized processing parameters such as stirring speed (250 rpm), stirring time (10 min) and preheating of reinforcing particles (250°C), pouring temperature 680°C and 2-stage addition of reinforcing particles by stir casting technique. Nearly, the similar values of process parameters have been noticed in some previous studies [11-15]. Typically, alumina particles tended to sink at a maximum pouring temperature, while at reduction in pouring temperature and speed of stirring, the higher rate of the addition of the particles into the molten metal leads to the agglomeration at the molten metal surface. Meanwhile, increasing the speed of stirring few particles were expelled at the outer periphery (external end) of the molten metal of the crucible due to the impeller wind and hence, incorporation of the particle is difficult to accomplish. If the temperature of the mold is reduced, the composite mixture solidified quickly and it is then difficult to transfer into the mold and also the required pressure could not be applied. This results in increased porosity of the produced composites. Suppose, if the mold temperature increased, alumina particles sunk to the bottom of the mold due to the low solidification rate and higher density of the alumina hence uniform dispersion of the particles is difficult to accomplish. Therefore, the uniform distribution of alumina particles is only achieved under the optimum process conditions which are discussed above.

The present study mainly deals with the preparation, characterization and evaluation of mechanical and fractographic properties of Al2014 alloy reinforced with different weight percentages (0, 9, 12, and 15) of alumina particles by using above mentioned optimized process parameters. The above selected optimized parameters led to the improved wettability and distributions of the alumina particles in the aluminium melt thereby, it helps to improve the mechanical properties of the produced composites after the addition of alumina particles with increase in weight percentage of reinforcing alumina particles.

EXPERIMENTAL DETAILS

The composites Al2014-Al$_2$O$_{3p}$, containing 9, 12 and 15 wt. % of Al$_2$O$_{3p}$ particulates, are synthesized in this research. The density of Al2014 is 2.8 g/cm^3 and that of Al$_2$O$_{3p}$ is 3.8 g/cm^3 [16]. The density of composites decreases with the addition of Al$_2$O$_{3p}$. The chemical composition, of Al2014 and properties Al2014 and Al$_2$O$_{3p}$ are shown in Tab. 1 and Tab. 2 respectively. For the present experiment, Al$_2$O$_{3p}$ with an average size of 88 µm are used (Supplied by Fenfee Metallurgical Pvt. Ltd Bangalore, Karnataka, India).

Elements (wt. %)	Si	Fe	Cu	Mn	Mg	Cr	Zn	Ti	Others	Al
Al 2014 alloy	0.68	0.19	4.48	0.82	0.62	0.02	0.18	0.05	0.04	bal.

Table1: The chemical composition of Al2014 alloy.

Properties	Density (g/cm^3)	Hardness (HB500)	UTS (MPa)	Elastic Modulus (GPa)
Al2014	2.8	135	483	70-80
Al$_2$O$_{3p}$	3.8	1175	665	300

Table 2: Properties of Al2014 alloy and Al$_2$O$_{3p}$ [16].

Al2014 alloy is charged into the heating furnace in order to liquidate the pre-calculated volume of Al2014 alloy. Normally, Al2014 alloy melts at 630°C; the melting furnace is superheated to 680°C. For temperature measurements thermocouples are used. The molten metal in the crucible is then degassed upto 2 minutes with the help of a hexa-chloro-ethane (C$_2$Cl$_6$) to extract the undesirable by-products. A ceramic material known as zirconia is coated (to avoid iron contamination) on the steel impeller used to stir the molten metal to form a vortex. The stirring process is conducted at a speed of 250 rpm and from the top of the melt; the impeller is plunged inside the melt of around sixty percent height of the molten metal. At the same time, the pre-calculated reinforcement quantity has been added into the vortex in two-stages to ensure a strong wet-ability agitation has been continued for up to ten minutes. The Al$_2$O$_{3p}$ reinforcing particles are pre-heated in the oven to 250°C, before being applied to the vortex of molten metal to extract the moisture content. Now, Al2014 alloy has been transferred into the solid cast iron mold along with 9 wt. % of Al$_2$O$_{3p}$ particles to get a composite after complete solidification. Likewise, Al2014-12 and 15 wt. % Al$_2$O$_{3p}$ composites are created for further experiments. Using the SEM instrument, the microstructural analysis is completed. Casting samples were examined and properly cleaned and etched by using Keller's reagent. According to ASTM E92-17, micro-hardness tests are performed on the composite produced at fifteen various places with the similar specimen using Micro-Vickers Hardness Tester (ZWICK/Roell-Indent Tester) with a load of HV 0.3 and a dwelling period 15 sec and an average of fifteen readings are considered. According to the ASTM E8 benchmark the tensile tests are carried out and for the tensile test the dimensions of the samples having a 9 mm gauge diameter and with a 45 mm gauge length.

RESULTS AND DISCUSSION

Characterization of the synthesized composites

Fig. 1 (a-d) depicts the microstructures of as-cast Al2014 and Al2014 with 9 weight percentage (Fig.1 b), 12 weight percentages (Fig.1 c) and 15 weight percentage (Fig.1 d) of alumina particles. The composite microstructure includes eutectic silicon and primary α-Al dendrites and, whereas particles of alumina are isolated between eutectic silicon and territories of the dendrites. The stirring of the melt at 250 rpm when adding preheated alumina particles in two phases have leads to the breakdown of the dendrite-shape into an equiaxed structure, thus improving the wettability and incorporation of particles of alumina in the liquefy and as well as it leads to dissemination (dispersion) of the alumina particles more consistently in the matrix. Fig. 1 (b-d) represents the dissemination of alumina particles in the produced composites at different weight percentage. Additionally the electron microphotographs demonstrate the alumina particles continue to isolate (segregate) and grouped (cluster) enriched by eutectic silicon in inter-dendritic areas at very few places as the weight percentages of alumina increases and this is mainly because of the choice of optimized processing

parameters during stir casting. Further, the electron microphotographs shows that the strengthened composite grain size (Fig.1 b-d) is smaller contrasted to the base alloy without alumina particles (Fig. 1 a) due to the introduction of the alumina particles into liquefy often serve as sites of heterogeneous nucleation throughout the solidification.

EDS analysis is carried out on as-cast Al2014, Al2014-9 and 15 wt. % of alumina reinforced specimens with a particle size of 88 μm which is demonstrated in Fig. 2 (a-c). The energy dispersive spectrograph for Al2014 as-cast (Fig. 2 a) which contains major alloying elements like Cu, Mg, Si, Ti, Mn, Fe and Zn and Fig. 2 (b) Al2014-9 wt. % of alumina composite clearly showed the presence of O, Mg, Si, Fe, Cu, Ti, Mn peaks in Al matrix and Fig. 2 (c) depicts the elemental analysis of Al2014-15 wt. % of Al_2O_{3p} composite which confirm the elements like O, Mg, Si, Cu, Ti and Mn in Al alloy matrix composite. Dispersion of alumina in Al2014 is confirmed by the existence of oxygen (O) peaks in Fig. 2 (b-c).
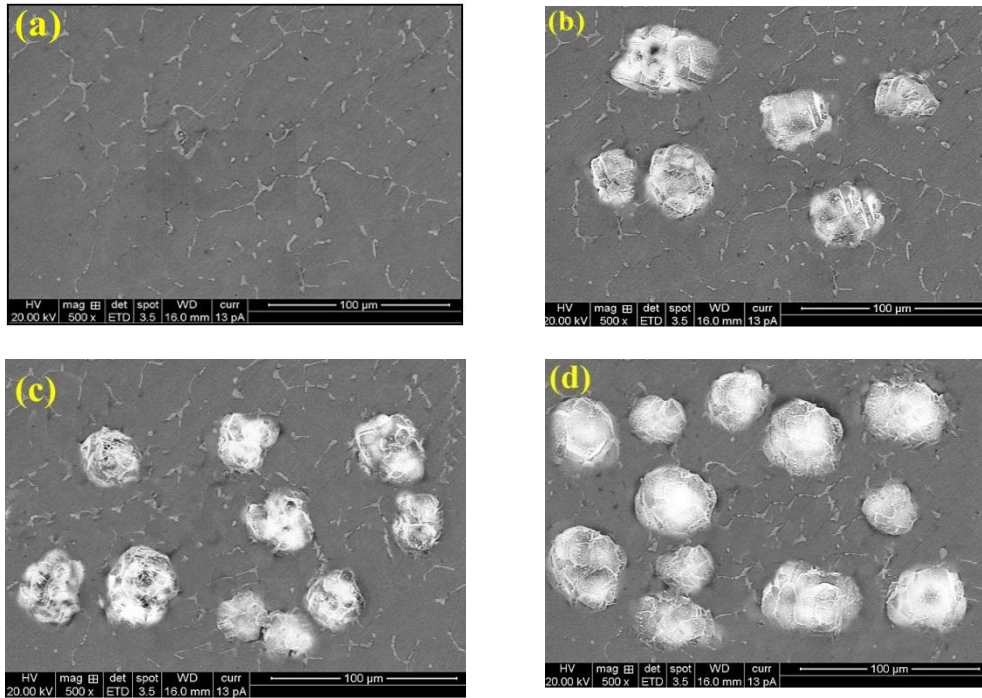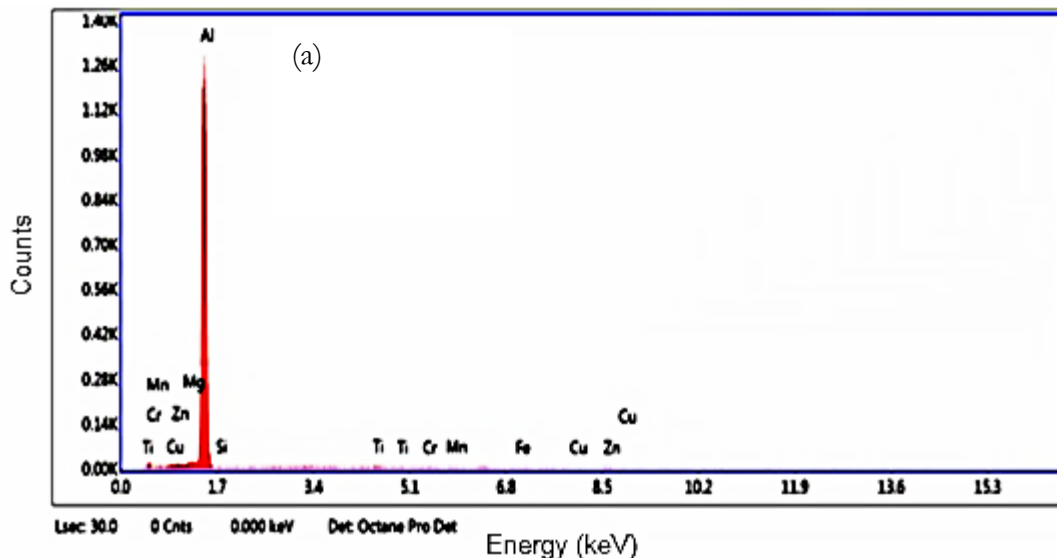

Figure 1: SEM images of Al2014-alumina (a) as-cast Al2014 alloy (b) Al2014-9 wt. % Al_2O_{3p} (c) Al2014-12 wt. % Al_2O_{3p} and (d) Al2014-15 wt. % Al_2O_{3p}.
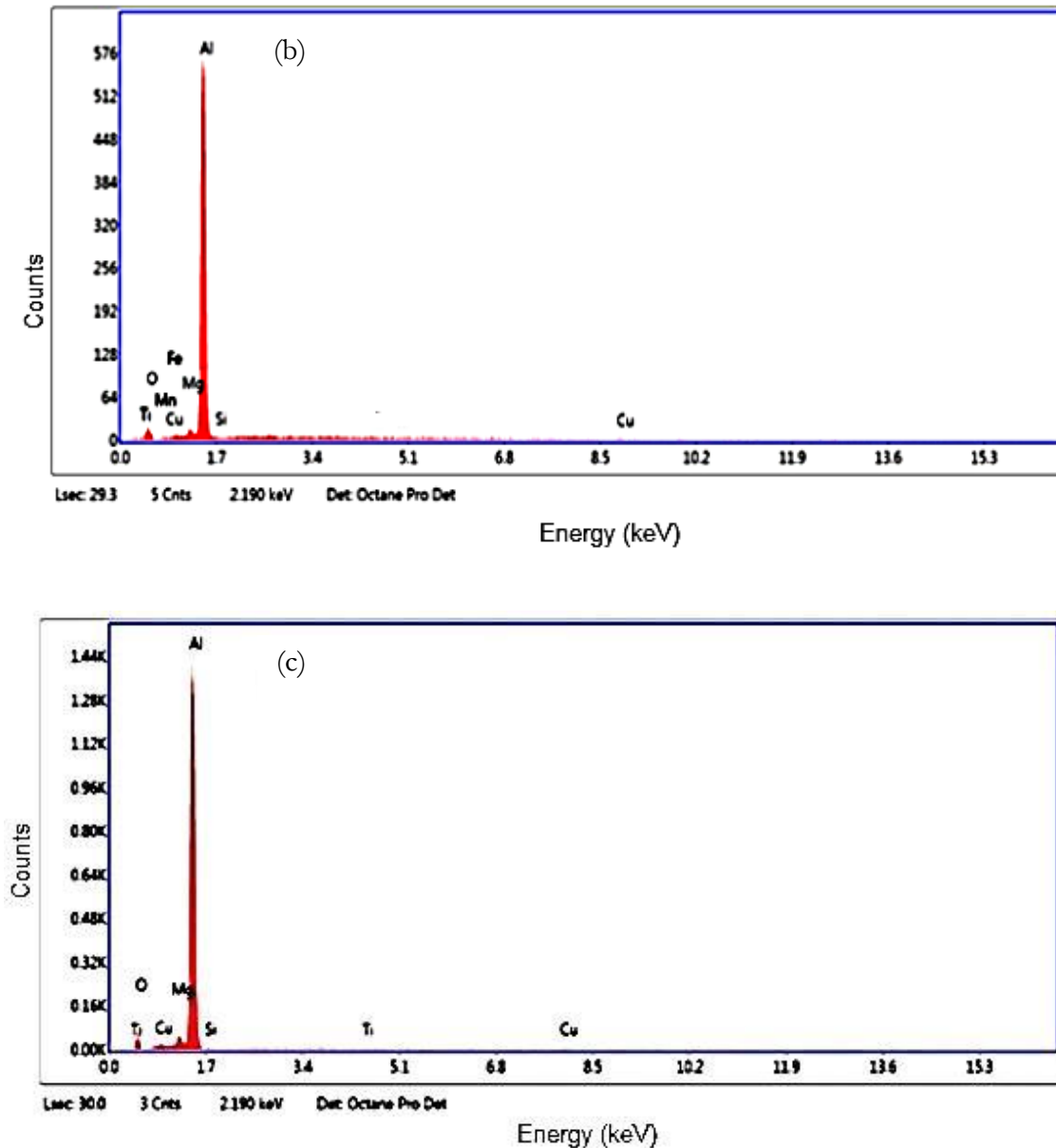
Figure 2: EDS spectrum of Al2014-Alumina (a) As-cast Al2014 (b) Al2014-9 wt. % Al_2O_{3p} and (c) Al2014-15 wt. % Al_2O_{3p} composites.

Hardness measurements
In the present work, micro-hardness is examined on base alloy (Al2014) and Al2014 reinforced alumina particles with different weight percentages (0, 9, 12, and 15). For each composite sample three specimens are produced and average values (w.r.t standard deviation) are graphically shown in Fig. 3.

Fig. 3 depicts the almost continuous increment in microhardness of the produced composite (Al2014-9, 12 and 15 wt. % Al_2O_{3p}) with increase in the weight percentage of alumina. The extent of improvement in the hardness of the produced composites is about 5.50, 13.17 and 19.20 percentages respectively as contrasted to Al2014 alloy. Enhancement in the matrix hardness is mainly because of existence of alumina [17, 18]. Basically strengthening (reinforcing) particles are stronger and more rigid than the matrix and these strengthening particles always try to avoid the plastic deformation of the matrix throughout the testing [17, 19-20]. But avoiding the plastic deformation of the matrix relies on the dissemination of the alumina particulates throughout the matrix. If the dissemination of the particles is clustered in a specific area and absence in small places might leads to the remarkable change in the hardness value at various locations in the composite samples. Among the above produced composite with different weight proportions, the composite

reinforced with Al2014-15 weight percentage of alumina particulate results in maximum hardness as compared to the as-cast Al2014 and composites produced with 9 and 12 weight percentage of alumina particulate composites.

In addition, no major cracks are found across the indentation, the pyramidal indentations are not damaged and despite the difference in hardness between hard reinforcing phase and soft matrix (Fig. 3). This suggests that the Al_2O_{3p} are strongly formed a bond to the Al matrix, that can play a key role in improving the composites mechanical properties.
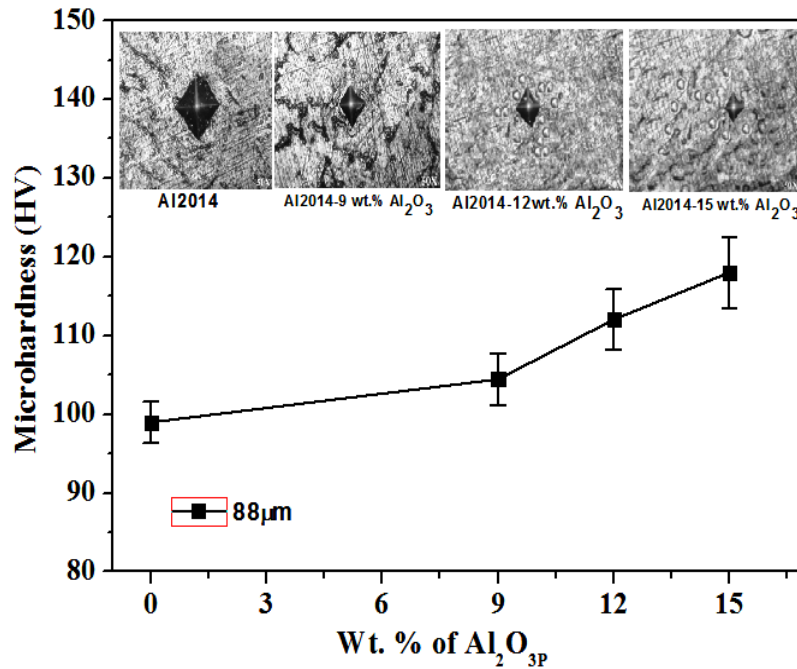

Figure 3: Micro-hardness values of Al2014 and Al2014 reinforced with alumina particles with different compositions

Evaluation of Ultimate Tensile Strength (UTS), Yield Strength (YS) and Percentage Elongation of synthesized composites

For the evaluation of tensile behaviors each composite sample three trials are conducted and average values (w.r.t standard deviation) are graphically shown in Fig. 4 (a-c). Fig. 4 (a-b) depicts the almost continuous increment in the UTS and YS of the produced composite with increase in the weight percentage of alumina. The extent of improvement in the UTS and YS of the produced composites is about 12.46, 16.29 and 29.59 percentages and 5.45, 12.46 and 29.54 percentages respectively as contrasted to Al2014 alloy. Tab. 4 and Fig. 4 (a) clearly reveals that improvements in UTS are obtained in Al2014 matrix after reinforcing with hard ceramic alumina particles.
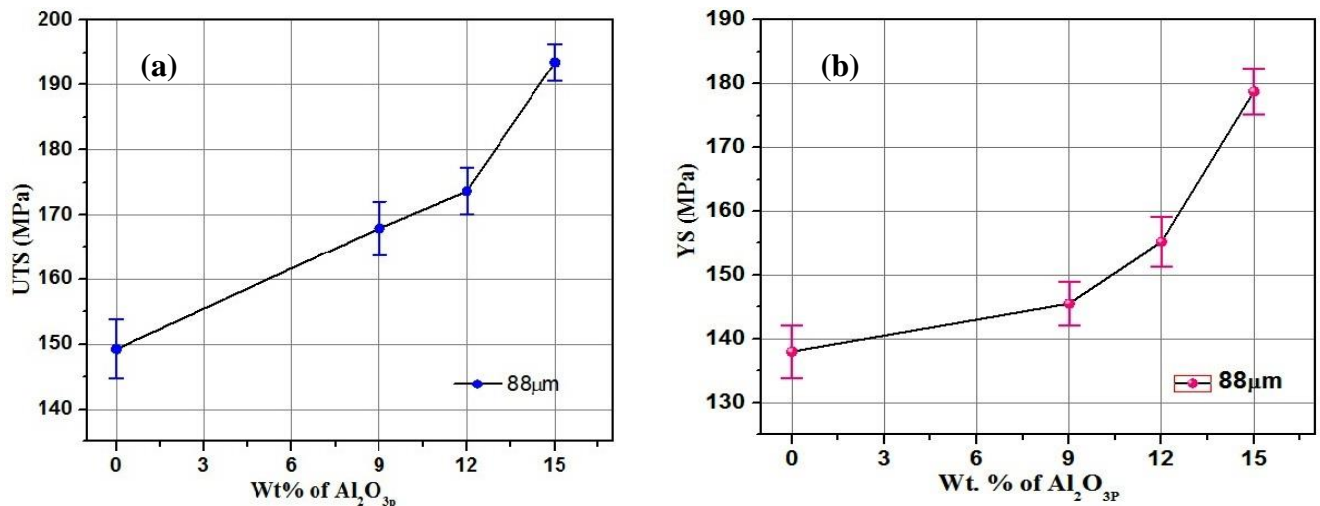

Figure 4: (a-b) UTS and YS values of Al2014 and Al2014 reinforced with alumina particles with different compositions
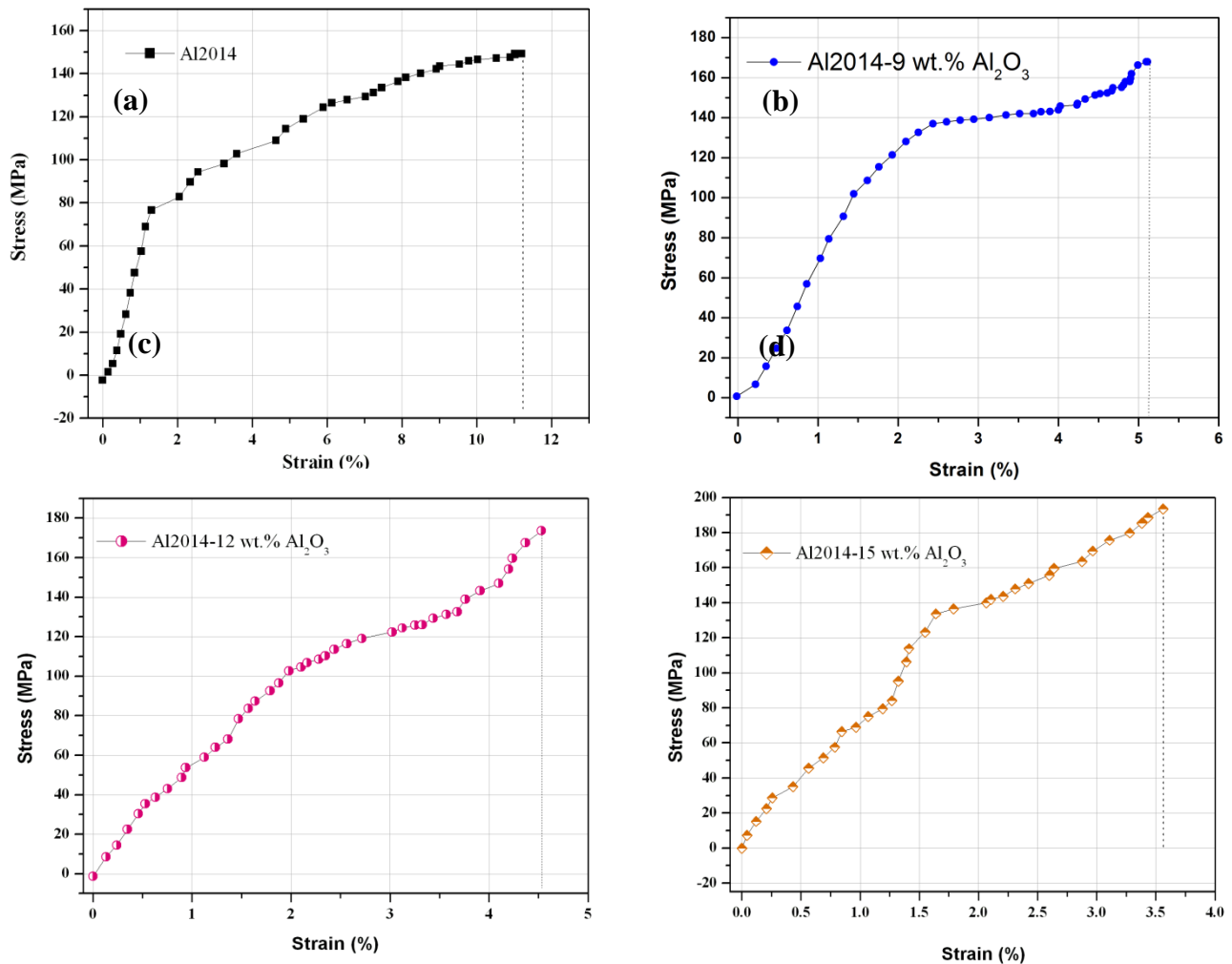
Figure 5: (a-d) Stress-strain curves for Al2014 and Al2014 reinforced with alumina particles with different compositions.

This enhancement is observed because of increasing the addition level of alumina particulates in the base alloy/ matrix (Al2014). Base alloy (matrix) strength is increased due to the incorporation of reinforcing particulates leading to higher resistance to the tensile stress and increases the overall tensile strength [21]. Furthermore, since the alumina particles are stiffer than the Al matrix, the alumina particles initially carry a large amount of stress. Furthermore, due to geometric restrictions imposed by the presence of reinforcement, the inclusion of alumina particles in the matrix alloy contributes to an improvement in the work hardening of the composite. This increases the tensile strength of the composite [22] by the load necessary for void nucleation and its propagation is more. As several studies [23, 24] reported that the particle size of the reinforced phase is extremely low, so the chances of having strength limiting faults or failures in the composite is anticipated to be lower, contributing to an improvement in the UTS. Also, it is obvious that the existence of alumina particles substantially increases the yield strength. This may have been attributed to the following factors (i) good interface strength among alumina reinforcement and Al2014 alloy as confirmed by electron microscopic images (i.e., Fig. 1 b-d). The possible reason for this because of the lower pores in the interface, which contributes considerably less failures to serve as the initiating positions of a crack (ii) the presence of hard ceramic particles, a dislocation deficiency occurs, leading to pile up of dislocations as a result a back stress is generated [3], since, the plastic deformation of the matrix resisting elastically deformed particles, back stress arises [25] (iv) in addition to the trapping of dislocation of second phase alumina particle matrix during deformations, thermal mismatch between Al matrix ($23 \times 10^{-6}/°C$) and ceramic Al_2O_{3p} ($8.2 \times 10^{-6}/°C$) contributes to increased dislocation density [26].

Fig. 5(a-d) shows the stress-strain relationship of the as cast Al2014 alloy matrix and the produced composites with different weight fractions. As increase in weight fraction of Al_2O_{3p} the fracture strain decreased and also the ductility of the produced composites was also decreased slowly due to the presence of alumina reinforcing particles which oppose the plastic flow of the matrix material.

Fig. 6 depicts the almost continuous decrements in the percentage elongation of the produced composite by increasing the weight percentage of alumina when contrasted with the cast Al2014 matrix alloy. The decrease in ductility is because of the following reasons (i) void nucleation by increasing addition level of reinforcement. The specific explanation for this difference may be that alumina particle behaves like a stress concentrator ii) the solid interfacial strength with reinforcement and matrix is extremely high, leading to greater reinforcement load, thus fracturing at lower strains [27]. Chandrasekhar and co-authors [28] have examined the tensile performance of Al-Al$_2$O$_{3p}$ composite and decline in the ductility is noticed with addition of hard reinforcement.
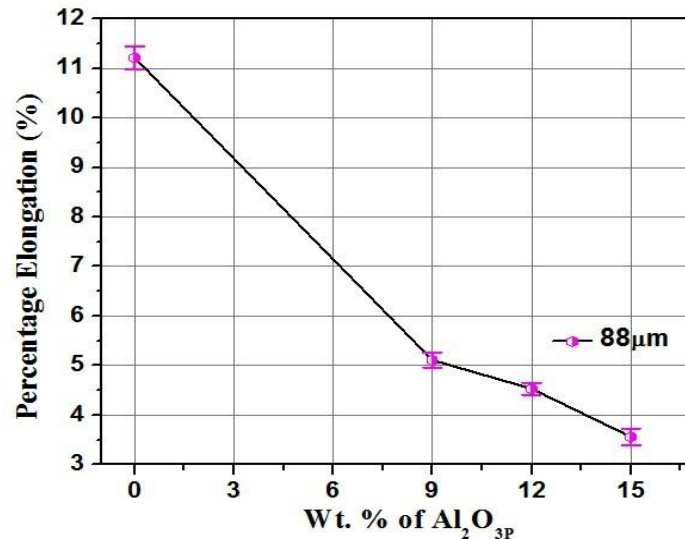

Figure 6: Percentage elongation values of Al2014 and Al2014 reinforced with alumina particles with different compositions

Fractography

To find the cause of failure of the materials produced, a study on the broken surface of the alloys and their composites is essential. During study of fractography, there are two important points to recall: a ductile material when it fails to produce small dimples, such as structure, in broken areas, while transgranular (grain fractures) or intergranular (grain boundary fractures), fragmentations may be found in SEM images taken out of a failed material, in case of fractured fractures.

Fig. 7 (a-d) illustrates the fractured surfaces of both as-cast Al2014 alloy and Al2014-9, 12 and 15 wt. % alumina particles. The base matrix displayed fine shallow and uniform dimples suggesting a ductile fracture, as is evident from Fig 7a, while the composite showed a two-way dimple distribution i.e., the reinforcing particles were taken up by the bigger dimples, while the ductile breakdown of the matrix induced smaller dimples. In addition, the SEM of the broken composite surface (Fig. 7b and Fig. 7d) showed hairline cracks on Al$_2$O$_{3p}$, partial decohesion among matrix and reinforcement and also matrix fracture. In most cases, particles were smooth in fracture surfaces suggesting that the particles are broken and not de-cohered and that these composites are dominated by their high interface strengths. The fracture surfaces in Al2014 matrix were divided between big dimples and while relatively smaller dimples were seen in composite reinforced with 12 and 15 wt % Al$_2$O$_{3p}$ (Fig. 7 c-d), indicating the mechanism for failure resulting from ductile void growth, coalescence and failure. Finally, the result is that the fracture behaviour of the Al2014 matrix changed from the ductile to the fragile modes and then to intermediate ductile mode because of the incorporation of Al$_2$O$_{3p}$. Small dimples are seen with the matrix and hairline crack in the Al$_2$O$_{3p}$ particles.

CONCLUSIONS

In the current work Al2014-Al$_2$O$_{3p}$ composites were successfully synthesized with 9, 12 and 15 wt. % of Al$_2$O$_{3p}$ with an average particle size of 88 μm by the utilization of stir casting technology. ASTM criteria refer to the microstructural study and significant mechanical performance such as hardness, UTS and YS, percentage elongation and fractography behaviour. As cast-alloy and equally distributed Al$_2$O$_{3p}$ in the prepared composite, the matrix is practically pores-free, as can be seen from SEM micrographs. The EDS analysis indicates that the Al2014 alloy matrix includes Al$_2$O$_{3p}$ particles. The mechanical properties of Al2014-9, 12 and 15 wt. % Al$_2$O$_{3p}$ composite are superior and improved

compared with unreinforced Al2014 as-cast material. The fracture surface of the synthesized composite material comprises of tiny voids owing to strain localization.
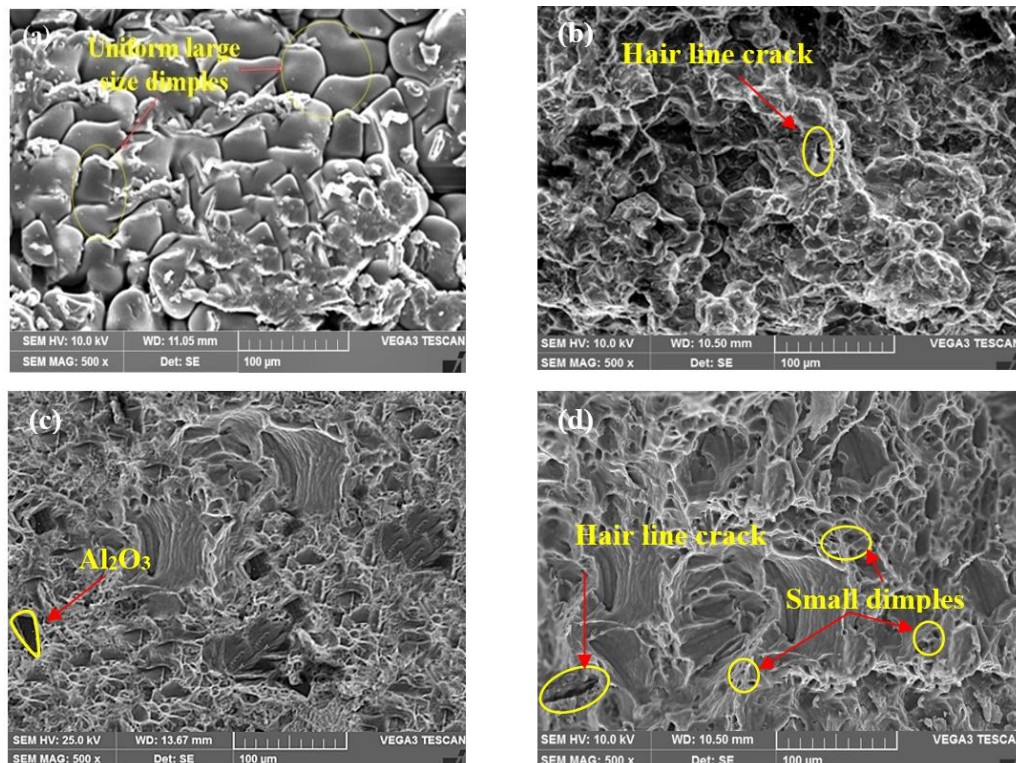

Figure 7: (a-d) Fractographs of images of (a) Al2014 and (b) Al2014-9 wt. % Al_2O_{3p} (c) Al2014-12 wt. % Al_2O_{3p} and (d) Al2014-15wt. % Al_2O_{3p}.

REFERENCES

[1] Sajjadi, S.A., Ezatpour, H.R. and Torabi Parizi, M. (2012). Comparison of microstructure and mechanical properties of A356 aluminum alloy/Al_2O_{3p} composites fabricated by stir and compo-casting processes. Materials and Design, 34, pp.106–111.

[2] Sajjadi, S.A., Torabi Parizi, M., Ezatpour, H. R. and Sedghi, A. (2012). Fabrication of A356 composite reinforced with micro and nanoAl_2O_{3p} particles by a developed compocasting method and study of its properties. Journal of Alloys and Compounds, 511, pp. 226–231.

[3] Sajjadi, S.A., Ezatpour, H.R. and Beygi, H. (2011). Microstructure and mechanical properties of Al–Al_2O_{3p} micro and nanocomposites fabricated by stir casting. Materials Science and Engineering A, 528, pp. 8765–8771.

[4] Li, G.R., Zhao, Y.T., Wang, H.M., Chen, G., Dai, Q.X. and Cheng, X.N. (2008). Fabrication and properties of in situ (Al3Zr + Al_2O_{3p})p/A356 composites cast by permanent mould and squeeze casting. Journal of Alloys and Compounds, 471, 04, 037.

[5] Alksandar, Vencl., Ilika, Bobic., Saioa, Arostegui., Biljana, Bobic., Aleksandar, Marinkovic. and Miroslav, Babic. (2010). Structural, mechanical and tribological properties of A356 aluminium alloy reinforced with Al_2O_3, SiC and SiC+ graphite particles. Journal of Alloys Compound, 506, pp. 631–639.

[6] Yung, C.K. and Chan, S.L.I. (2004). Tensile properties of nanometric Al_2O_3 particulate reinforced aluminium matrix composites. Journal of Materials Chemistry and Physics, 85, pp. 438-443.

[7] Chawla, N. and Shen, Y.L. (2001). Mechanical behavior of particle reinforced metal matrix composites. Advanced Engineering Materials, 3, pp. 357-370.

[8] Kheder, A.R.I., Marahleh, G.S. and Al-Jamea, D.M.K. (2011). Strengthening of aluminum by SiC, Al_2O_3 and MgO. Jordan Journal of Mechanical and Industrial Engineering, ISSN 1995-6665, pp. 533-541.

[9] Zhiqiang. Y.U. (2005). Microstructure and tensile properties of yttria coated-alumina particulates reinforced aluminum matrix composites. Journal of Material Science and Technology, Vol. 21, No.1.

[10] Kok, M. (2005). Production and mechanical properties of Al_2O_3 particle-reinforced 2024 aluminium alloy composites. Journal of Materials Processing Technology, 161, pp. 381–387.

[11] Hanumanth, G.S. and Irons, G.A. (1993). Particle incorporation by melt stirring for the production of metal-matrix composites. Journal of Material Science, 28, pp. 2459–2465.

[12] Seo, Y.H. and Kang, C.G. (1995).The effect of applied pressure on particle dispersion characteristics and mechanical properties in melt-stirring squeeze-cast SiC/Al composites. Journal of Material Processing Technology, 55, pp. 370–379.

[13] Milliere, C. and Suery, M. (1998). Fabrication and properties of metal matrix composites based on SiC fibre reinforced aluminium alloys. Material Science and Technology, 4, pp. 41–51.

[14] Hung, N.P., Boey, F.Y.C., Khor, K.A., Oh, C.A. and Lee, H.F. (1995). Machinability of cast and powder-formed aluminum alloys reinforced with SiC particles. Journal of Materials Processing and Technology, 48, pp. 291–297.

[15] McLean, A., Soda, H., Xia, Q., Pramanick, A.K., Ohno, A., Motoyasu, G., Shimizu, T., Gedeon, S.A. and North, T. (1997). SiC particulate-reinforced, aluminium-matrix composite rods and wires produced by a new continuous casting route. Composites, Part A, 28, pp. 153–162.

[16] ASM Handbook. (1990). ASM handbook Committee, pp 62–122. DOI: 10.1361/asmhb a0001 060.

[17] Bharath, V., Nagaral, M., Auradi, V. and Kori, S, A. (2014). Preparation of 6061Al–Al_2O_3p MMCs by stir casting and evaluation of mechanical and wear properties. Procedia Materials Science, 6, pp. 1658–1667.

[18] Mittal, P. and Dixit, G. (2016). Dry sliding wear behaviour of 2014 aluminium alloy reinforced with SiC composite. International Journal of Engineering Research and Technology, 5, pp. 147–153.

[19] Bharath, V., Santrust, A., Madeva, Nagaral., Auradi, V. and Kori, S.A. (2018). Characterization and mechanical properties of 2014 aluminum alloy reinforced with Al_2O_3p composite produced by two-stage stir casting route. Journal of The Institution of Engineers (India): Series C, 100, pp. 277–282.

[20] Bharath, V., Madeva, Nagaral., Auradi, V. and Kori, S.A. (2020). Experimental investigations on mechanical and wear behaviour of 2014Al-Al2O3p Composites. Journal of Bio and Tribo-Corrosion, Springer Publication, pp. 1-10, DOI: 10.1007/s40735-020-00341-2.

[21] Gupta, M. (1999). Interrelationship between cumulative volume fraction of SiC particulates and porosity with ductility of Al/SiC composites. Aluminum Transactions, 1, 1, pp. 33-39.

[22] Chawla, N. and Shen, Y, L. (2001). Mechanical behavior of particle reinforced metal matrix composites. Advanced Engineering Materials, 3, pp. 357-370.

[23] Lewandowski, J.J., Liu, D.S. and Liu, C. (1991). Observations on the effects of particulate size and superposed pressure on deformation of MMCs. Scr. Metall., 25, pp 21-26.

[24] Kamat, S.V., Hirth, J.P. and Meharabian, R. (1989). Mechanical properties of particulate-reinforced aluminum-matrix composites. Acta Metallurgica, 37, pp. 2395-2402.

[25] Vikram Singh, Gaharwar. and Umashankar, V. (2014). The characterization and behavior of Al2014 reinforced with Al_2O_3p by powder metallurgy. Material Science and Engineering A, 6, pp. 3272-3275.

[26] Modi, O.P. (2014). Two-body abrasion of a cast Al–Cu (2014 Al) alloy–Al_2O_3p particle composite: influence of heat treatment and abrasion test parameters. Wear. 248, pp. 100 2001.

[27] Mahon, G.J., Jowe, J.M. and Vasudevan, A.K. (1990). Microstructural development and the effect of interfacial precipitation on the tensile properties of an aluminum/silicon-carbide composite. Acta Metallurgica et Materialia, 38, 1503. DOI: 10.1016/0956-7151(90)90118-Z.

[28] Chandrashekar, A., Ajaykumar, B.S. and Reddappa, H.N. (2018). Mechanical, structural and corrosion behavior of AlMg4.5-nano Al_2O_3p metal matrix composites. Materials Today Proceedings, 5, pp. 2811-2817.